Published by Institute of Physics Publishing for SISSA

Received: *August 29, 2005*
Accepted: *October 11, 2005*
Published: *October 26, 2005*

Time lumps in nonlocal stringy models and cosmological applications

Iirina Ya. Aref'eva

Steklov Mathematical Institute, Russian Academy of Sciences
Gubkin st. 8, Moscow, 119991, Russia
E-mail: arefeva@mi.ras.ru

Liudmila V. Joukovskaya

Steklov Mathematical Institute, Russian Academy of Sciences
Gubkin st. 8, Moscow, 119991, Russia, and
MSI, Växjö University
SE-351 95, Sweden
E-mail: ljoukov@mi.ras.ru

Abstract: We study lump solutions in nonlocal toy models and their cosmological applications. These models are motivated by a description of D-brane decay within string field theory framework. In order to find cosmological solutions we use the simplest local approximation keeping only second derivative terms in nonlocal dynamics. We study validity of this approximation in flat background where time lump solutions can be written explicitly and work out the validity of this approximation. Finally, we show that our models at large time exhibit the phantom behaviour similar to the case of the string kink.

Keywords: String Field Theory, D-branes, Tachyon Condensation.

JHEP10(2005)087

Contents

1. Introduction

In the last years strings and D-branes attracted cosmological applications related with the cosmological acceleration [1]–[5]. The observations suggest that the Universe is presently accelerating [6, 7]. It is believed that a new physics is required to explain this phenomenon. The bulk of energy density in the Universe is gravitationally repulsive and can be represented as an unknown form of energy (dark energy) with negative pressure and

negative equation of state parameter $w = p/\rho$. The current experimental data show that w lies in the range $-1.61 < w < -0.78$ [8−10]. There are various theoretical models — a quintessence scalar field [11], Dirac-Born-Infeld action [1]–[3], and other which are able to describe the case $w > -1$.

The most exciting possibility would be the case $w < -1$ (see [11]–[23], [5] and references therein). There are several phenomenological models describing this phantom Universe [13, 15]. In these models week energy conditions $\rho > 0, \rho + p > 0$ are violated and most of them are unstable and strange phenomena related with unstability appear [17]. There are also models related with modified gravity [24], but there is a problem of getting these models basing on fundamental principles.

Recently it was shown that the string field theory (SFT) description of D-brane decay leads at large times to an effective phantom model [5]. As a result of this decay the spectrum becomes stable and the model does not suffer from instability problems. D-brane decay in non-flat metric within the SFT framework is described by the string tachyon action [5]

$$S=\int\sqrt{-g}d^4x\left(\frac{\alpha'}{16\pi G}R+\frac{1}{g_0^2}(-\frac{\kappa^2}{2}g^{\mu\nu}\partial_\mu\phi\partial_\nu\phi+\frac{1}{2}\phi^2-U(\Phi))\right), \tag{1.1}$$

Here it is supposed that we deal with 3-dimensional D-brane, G is a 4-dimensional gravitational constant, α' is a string tension, $g_{\mu\nu}$ is a metric for dimensionless coordinates, R is a curvature, g_0 is a dimensionless string coupling constant, fields ϕ and Φ are dimensionless fields related via

$$\Phi=\exp\left(\frac{\beta}{2}\Box_g\right)\phi,\qquad \Box_g=\frac{1}{\sqrt{-g}}\partial_\mu\sqrt{-g}g^{\mu\nu}\partial_\nu\,, \tag{1.2}$$

β and κ^2 are constants whose values depend on the type of a string under consideration. The form of the potential also depends on the type of a string.

Action (1.1) in the Friedmann background

$$ds^2=-dt^2+a^2(t)(dx_1^2+dx_2^2+dx_3^2)\,, \tag{1.3}$$

gives Friedman equations and the equation for the field $\Phi=\Phi(t)$ which in turn reads as

$$\left(\kappa^2\mathcal{D}+1\right)e^{-\beta\mathcal{D}}\Phi=U'(\Phi)\,, \tag{1.4}$$

where $\mathcal{D}=-\partial_t^2-3H(t)\partial_t$, $H=\dot{a}/a$ is a Hubble parameter and $U'(\Phi)=\partial U/\partial\Phi$.

To study solutions of equation (1.4) the following approximation was used

$$(-\kappa^2+\beta\kappa_0^2)(\ddot{\Phi}+3H\dot{\Phi})=V'(\Phi)\,, \tag{1.5}$$

$$V(\Phi)=U(\Phi)-\frac{1}{2}\Phi^2\,, \tag{1.6}$$

κ_0^2 is a parameter close to 1. This second order derivatives approximation is called mechanical or local approximation. In a rather rough approximation one can take $\kappa_0^2\simeq 1$ (a so-called direct mechanical approximation).

For $\beta\kappa_0^2>\kappa^2$ we get ghost kinetic term in (1.5). For this case after time rescaling we can take $\beta\kappa_0^2-\kappa^2=1$. This case corresponds to a phantom model. The dynamics of the phantom model in the flat background reproduces dynamics of the usual particle in the overturn potential [35]. The equation of state parameter w for the phantom in a general potential can be represented as

$$w=-1-\frac{1}{3m_p^2}\frac{\dot{\Phi}^2}{H^2}\,, \tag{1.7}$$

where m_p^2 is a dimensionless parameter related with the Plank mass M_p^2, $m_p^2=M_p^2\alpha'=\alpha'/8\pi G$.

JHEP10(2005)087

For a cubic potential U the action (1.1) is the curved version of the action for the tachyon field in the Witten SFT [25] at the lowest order in the level truncation scheme [26, 27]. It is supposed that we deal with 3-dimensional D-brane in 26-dimensional space-time and the volume of compactified 22-dimensional space in (1.1) is omitted.

For a quartic U the action (1.1) is the curved version of the action for the tachyon field which was obtained in an approximation of slow varying auxiliary field [35] from cubic fermionic SFT[28]. This action in the flat case has been obtained for the case when the string field contains only two fields: the tachyon in the GSO(-) sector[1] and a lowest auxiliary field in the GSO(+) sector. Integration over this auxiliary field produces a fourth degree of the tachyon self interaction.

The existence of the kink solution for the flat version of equation (1.4) with $\kappa = 0$ has been shown numerically in [37] and has been proved in [39]. A validity of the approximation (1.5) for this kink solution has been studied in [38].

In the case of the flat metric and $\kappa = 0$ the kink solution of (1.4) is a monotonic function interpolating between two different vacuum solutions. However not only monotonic kink solutions appear in the dynamics of string tachyons. For $\kappa \neq 0$, $\kappa^2 < \beta\kappa_0^2$ and $H = 0$ there are non-monotonic kink solutions of (1.4) and these solutions have bounce points. In the open-closed string model [40] a bounce point also appears [41]. Typical examples of solutions with one bounce point are lump solutions. In particular, such type of solutions has been recently found in [42].

In this paper we consider two SFT inspired models with the action (1.1). For the first model

$$U = \frac{\sqrt{k}}{k+1}\Phi^{k+1}, \qquad k < 1, \tag{1.8}$$

and for the second model the potential is a special polynomial

$$U = \sum_{n=1}^{N} \frac{\alpha_n}{n+1}\Phi^{n+1}. \tag{1.9}$$

Distinguished feature of these models is that they have explicit lump solutions for $\kappa = 0$ in flat background. We study a validity of the mechanical approximation to these solutions. For this purpose we compare essential physical characteristics such as energy and pressure of the nonlocal systems with their mechanical analogues. We find that under special conditions these characteristics in both models are rather similar. Also in both cases it is possible to find small explicit modifications of the mechanical potentials to solve corresponding local equations in the Friedmann metric.

The paper is organized as follows. In section 2 we consider the equation of motion

$$e^{\beta\partial_t^2}\Phi = \sqrt{k}\Phi^k. \tag{1.10}$$

where $0 < k < 1$, $a > 0$. There is the lump solution to this equation

$$\Phi(t) = e^{-\xi t^2}, \qquad \xi = \frac{1-k}{4\beta k}. \tag{1.11}$$

The energy of the solution (1.11) is equal to zero.

[1] To produce nonBPS-branes the GSO(-) sector is involved [29, 30] (see reviews [31]–[33] for details).

In section 2.2 we compare (1.11) with zero energy periodic trajectories in the direct mechanical approximation of (1.5). The period T_k becomes large when $k \to 1$. We show that for time $t < T_k/2$ the zero-energy periodic solutions to the mechanical problem rather well approximate the lump solution (1.11).

In section 2.3 we calculate explicitly the pressure on the solution (1.11) and in section 2.4 compare it with the pressure of the zero-energy periodic solution of the mechanical problem for $|t| < T_k$. We find that the mechanical approximation represents a behavior of the pressure of the non local problem with a good degree of accuracy for k closed to 1, $k < 1$. We also compare Φ with $\tilde{\Phi} = e^{\beta/2\partial_t^2}\Phi$ and conclude that a comparison of Φ and $\tilde{\Phi}$ gives a rather good quantitative criterium for a validity of the local approximation. A precise condition of a validity of the local approximation is a condition that the magnitude of $\tilde{\Phi} - \Phi - \frac{\beta}{2}\partial_t^2\Phi$ is small.

In section 3.1 we consider a modified integral equation with the constant friction

$$e^{\beta\partial_t^2 + h\partial_t}\Phi_h = \sqrt{k} g(t)\Phi_h^k\,, \tag{1.12}$$

and special time depending coupling constant $g(t) = e^{-2h(1-k)t}$. (1.12) has an explicit lump solution

$$\Phi_h(t) = e^{-\xi t^2 + Bt}\,, \qquad B = \frac{h}{2\beta}\left(-1 - \sqrt{1 + 16\xi\beta^2}\right). \tag{1.13}$$

We see that the friction makes behavior of the solutions of the nonlocal equation more closed to that of the corresponding mechanical problem. This give us a possibility to use this approximation for Friedmann equations.

In section 3.2 we study numerically the corresponding Friedmann equations and find that there is a regime, i.e. suitable initial conditions, that represents an acceleration with $w < -1$.

In section 3.3 we reconstruct explicitly the potential for which (1.11) is an exact solution of the Friedman equations. This potential has the form

$$V(\Phi) = V_0(\Phi) + V_1(\Phi)\,, \tag{1.14}$$

where

$$V_0(\Phi) = -2\,\xi\,\Phi^2\,\log\Phi\,, \tag{1.15}$$

and $\delta V(\Phi)$ is of order of $1/m_p^2$.

$$V_1(\Phi) = \frac{3\,\xi}{64 m_p^2}\left(\sqrt{2\pi}\,\mathrm{e}\;rf(\sqrt{-2\log\Phi}) - 4\Phi^2\,\sqrt{-\log\Phi}\right)^2.$$

In section 4 we search for lump solutions of the following equation

$$e^{\beta\partial^2}\Phi = \sum_{n=1}^{N}\alpha_n\Phi^n\,, \tag{1.16}$$

where α_n are constant. It is know that a direct numerical search for lumps solutions is a rather difficult problem. There are also nonexistence theorems for a wide class of potentials[36, 39]. It is also interesting to find lump as well as kink solutions in vacuum SFT [43, 44].

Here we accept the following strategy. We start from a given function

$$\varphi_0(t) = \mathrm{sech}^2(t) \tag{1.17}$$

and find constant α_n from a requirement that the function (1.17) is a solution to equation (1.16) with a small discrepancy for fixed N. We mean that the discrepancy has a small L_2-norm. We consider the cases $N = 3, \ldots, 14$. Qualitatively one can say that lowest coefficients α_n show a stable picture when $N \to \infty$. With the obtained α_n in section 4.2 we find numerical solutions to (1.16) with zero energy using an analog of Freedman method (see [41] and references therein).

Then in section 4.3 we study a mechanical approximation to equation (1.16). It occurs that all potentials V have local maximum at $\Phi = 0$ and are equal to zero at Φ_{0N}, $\Phi_{0N} < 1$ and $\Phi_{0N-1} \simeq \Phi_{0N}$. As has been mentioned above, the lowest coefficients α_n are stabilized as $N \to \infty$. For the zero-energy solutions of the mechanical problem with the initial data $\Phi(0) = \Phi_{0N}$ one has $|\Phi(t)| < 1$ and for such Φ only the low-order coefficients dominate in the potential. Therefore, in spite of global change of the behavior of potentials with N increasing, the form of potentials near the region, where the particle with the above initial data moves, does not change. For small time trajectories of the mechanical problems with above mentioned initial data do not reproduce the lump (1.17) since $\mathrm{sech}^2(t)$ has derivatives of the same order as itself. However for large time when trajectories are closed to an attractor point $\Phi = 0$ they are also closed to the lump.

The profile of the potential (1.6) with found α_n in the region $0 < \Phi < 1$ is rather closed to the profile of the potential

$$V_0(\Phi) = 2\,(1-\Phi)\,\Phi^2 \tag{1.18}$$

for which the function (1.17) solves the mechanical problem with the lump boundary conditions. In section 4.5 we show that engaging of the Friedmann metric modifies the potential (1.18) and one has to add

$$V_1 = -\frac{4}{75 m_p^2}(-1+\Phi)^3\,(2+3\Phi)^2$$

to (1.18) in order the function (1.17) to be a solution of the Friedmann equations.

2. Gaussian lump

2.1 Action and equation of motion

In this section we consider the action

$$S = \int d^d x \left[\frac{1}{2}\phi^2 - \frac{\sqrt{k}}{k+1}\Phi^{k+1}\right], \tag{2.1}$$

with an unusual non-polynomial interaction

$$0 < k < 1 \tag{2.2}$$

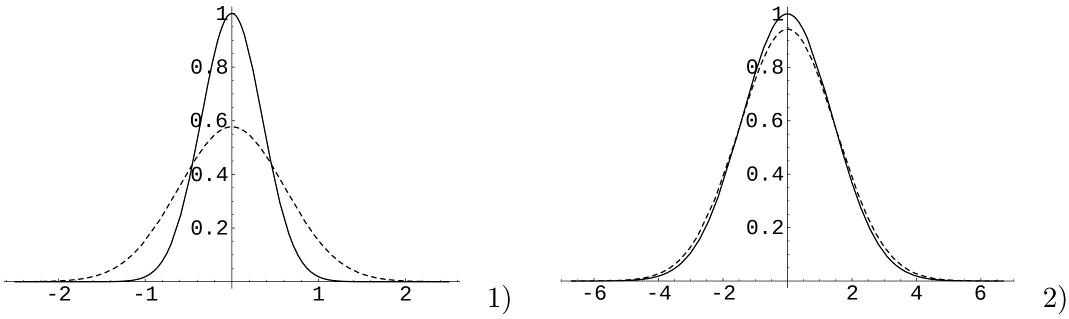

Figure 1: Solutions of integral equation (2.5): 1) for $\beta = \frac{1}{4}$, $k = 0.2$; 2) for $\beta = \frac{1}{4}$, $k = 0.8$. The firm line is Φ and the dashing line is ϕ.

and where $\Box = -\partial^2 + \nabla^2$,

$$\Phi(x) = e^{\frac{\beta}{2}\Box}\phi(x)\,, \qquad a > 0\,. \tag{2.3}$$

The equation of motion for this action is

$$e^{-\beta\Box}\Phi(x) = \sqrt{k}\Phi^k\,. \tag{2.4}$$

For space homogeneous configurations $\Phi = \Phi(t)$ it takes the form

$$e^{\beta\partial^2}\Phi(t) = \sqrt{k}\Phi^k(t)\,, \tag{2.5}$$

here and below $\partial = \partial_t$.

Equation (2.4) has the following solution

$$\Phi(t) = e^{-\frac{b}{4\beta}t^2}\,, \qquad b = \frac{1-k}{k}\,. \tag{2.6}$$

The relation between Φ and ϕ is

$$\Phi(t) = e^{-\frac{\beta}{2}\partial^2}\phi(t) \tag{2.7}$$

and one can get ϕ from Φ using the smoothing integral representation

$$\phi(t) = \frac{1}{\sqrt{2\pi}}\int e^{-\frac{(t-t')^2}{2\beta}}\Phi(t')dt'\,. \tag{2.8}$$

Substituting (2.6) into (2.8) one gets smoothed solution ϕ

$$\phi(t) = \frac{\sqrt{2}}{\sqrt{2+b}}e^{-\frac{b}{2\beta(2+b)}t^2}\,. \tag{2.9}$$

From (2.6) and (2.9) we see that Φ and ϕ are related as

$$\phi(t) = \sqrt{c}\Phi(\sqrt{c}t)\,, \qquad \text{where } c = \frac{2k}{1+k}\,. \tag{2.10}$$

When $k \to 1$, $c \to 1$ and therefore $\phi \cong \Phi^2$ and when $k \to 0$, $c \to 0$ and $\phi \cong 0$. This is illustrated on figure 1 where solutions of (2.5) and corresponding smoothed fields ϕ are presented for different values of k.

[2]Let us note that in the more complicated model [40] ($c_2 = \frac{13}{6}$) it is known, that physical (analog of ϕ) and tilded (analog of Φ) fields coincide with very high precision [41].

JHEP10(2005)087

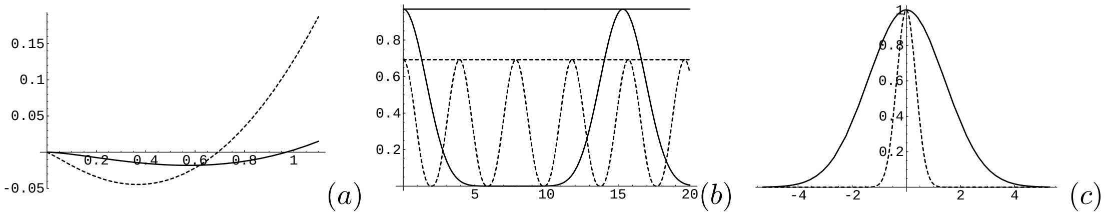

Figure 2: (a) The potential V for the k= 0.2 (dashing line) and for k=0.8 (firm line). (b) The numerical solution of equation (2.11) for k=0.2 (dashing line) and for $k = 0.8$ (firm line). (c) Exact solution to integral equation (2.5) for $\beta = 1/4$ and k= 0.2 (dashing line) and k=0.8 (firm line).

k	$1/5$	$1/3$	$1/2$	$2/3$	$8/9$	$9/10$
T	$5\pi/4$	$3\pi/2$	2π	3π	9π	10π

Table 1: Periods T_k (2.13) for various k with $\beta = 1/4$.

JHEP10(2005)087

2.2 Mechanical approximation

Let us consider the mechanical approximation for equation (2.5),

$$\beta\ddot{\varphi}(t) = -V'_{ot}(\varphi)\,, \tag{2.11}$$

the parameter β plays a role of mass of the particle. The potential V_{ot} is an overturn version of the potential (1.6) for U given by (1.8),

$$V_{ot}(\varphi) = -V(\varphi)\,, \qquad V(\varphi) = \frac{\sqrt{k}}{k+1}\varphi^{k+1} - \frac{1}{2}\varphi^2\,. \tag{2.12}$$

To have a real potential V in (2.12) let us assume that $k = 1 - 2\delta$ and present the corresponding square in U as $(\Phi^2)1/(1-\delta)$. In this case the potential $V_{ot}(\Phi)$ is an even function and this function is equal to zero at $\Phi = 0$ and has beak with singular second derivative $\Phi = 0$, see figure 2a. The particle with the zero energy oscillates between the point $\varphi = 0$ and the bounce at $\varphi_{\max} = (\frac{2\sqrt{k}}{1+k})^{\frac{1}{1-k}}$. The zero-energy trajectories are presented in the figure 2b and the exact lumps (2.6) are presented on figure 2c for different k.

The periods of these motions are

$$T_k = \sqrt{\beta}\int_0^{\varphi_{\max}} \frac{d\varphi}{\sqrt{-2V_{ot}}}\,. \tag{2.13}$$

In the table 1 we enumerate values of T for different k and $\beta = 1/4$.

The solutions of the integral equations (2.5) (see figure 2c) and their mechanical analogs (2.11) describe different physical behavior. Namely, the solution (2.6) of the integral equation starts from zero go above the bounce point $\varphi_{\max}$ then rises $\Phi = 1$ and returns to zero. Thus the solution of the integral equation does not bounded by the bounce point, whereas the zero-energy solution of the mechanical model presents a periodic motion between the bounce point and zero. The period depends on k and as k goes to 1 the period becomes infinite, i.e. $k = 1$ corresponds to the free motion. Therefore, for small $k \ll 1$ the mechanical approximation does not work, while it works for $t < T_k$ for k goes to 1.

2.3 Energy and pressure

In this subsection we consider the energy and the pressure of the nonlocal problem (2.5) and compare them with energy and pressure of the corresponding mechanical problem (2.11). Equation (2.4) has the conserved energy (compare with [35])

$$E = E_p + E_{nl_1} + E_{nl_2}\,, \tag{2.14}$$

where

$$E_p = -\frac{1}{2}\phi^2 + \frac{\sqrt{k}}{k+1}\Phi^{k+1}\,, \tag{2.15}$$

$$E_{nl_1} = \frac{\beta}{2}\int_0^1 \left(e^{-\frac{\beta}{2}\rho\partial^2}\sqrt{k}\Phi^k\right)\left(e^{\frac{\beta}{2}\rho\partial^2}\partial^2\Phi\right)d\rho \tag{2.16}$$

and

$$E_{nl_2} = -\frac{\beta}{2}\int_0^1 ((e^{-\frac{\beta}{2}\rho\partial^2}\sqrt{k}\partial\Phi^k))(e^{\frac{\beta}{2}\rho\partial^2}\partial\Phi)d\rho\,. \tag{2.17}$$

One can see that this energy conserves. Indeed,

$$\begin{aligned}\frac{dE(t)}{dt} &= -\phi\partial\phi + \sqrt{k}\Phi^k\partial\Phi + \frac{\beta}{2}\int_0^1 \left(e^{-\frac{\beta}{2}\rho\partial^2}\sqrt{k}\Phi^k\right)\overleftrightarrow{\partial}\left(e^{\frac{\beta}{2}\rho\partial^2}\partial\Phi\right)d\rho \\ &= -\phi\partial\phi + \sqrt{k}\Phi^k\partial\Phi - \sqrt{k}\Phi^k\overleftrightarrow{e^{-\frac{\beta}{2}\partial^2}}\partial\phi = \partial\phi\left[-\phi + e^{-\frac{\beta}{2}\partial^2}\sqrt{k}\Phi^k\right] = 0.\end{aligned}$$

The pressure in the model (2.1) has the form

$$P = E_{nl_2} - E_p - E_{nl_1}\,. \tag{2.18}$$

Substituting in this formula expressions for E_{nl_1} and E_{nl_2} given by (2.16) and (2.17) one gets

$$P = -\beta\int_0^1 (e^{(2-\rho)\frac{\beta}{2}\partial^2}\partial\Phi)(e^{\frac{\beta}{2}\rho\partial^2}\partial\Phi)d\rho\,. \tag{2.19}$$

Substituting in (2.19) the explicit form of the solution (2.6) we get

$$P = -\frac{2b^2t^2}{\beta}\int_0^1 \frac{d\rho}{[(2-b(\rho-2))(2+b\rho)]^{\frac{3}{2}}}\ \exp\left(-\frac{t^2}{\beta}\frac{b(2+b)}{4+4b-b^2(\rho-2)\rho}\right). \tag{2.20}$$

From formula (2.20) we see that the pressure is negative and for large time goes to zero.

2.4 Compression of pressure for nonlocal and local problems

Comparing expressions (2.14) and (2.18) with standard expressions of the energy and pressure for a scalar field, $E_\varphi = \frac{1}{2}\dot{\varphi}^2 + V(\varphi)$, $P_\varphi = \frac{1}{2}\dot{\varphi}^2 - V(\varphi)$, one can say that E_{nl_1} and E_{nl_2} play roles of extra terms in the nonlocal “kinetic’ energy $\mathcal{E}_k$ and ’potential” energy $\mathcal{E}_p$, i.e.

$$E = \mathcal{E}_k + \mathcal{E}_p \tag{2.21}$$

$$P = \mathcal{E}_k - \mathcal{E}_p \tag{2.22}$$

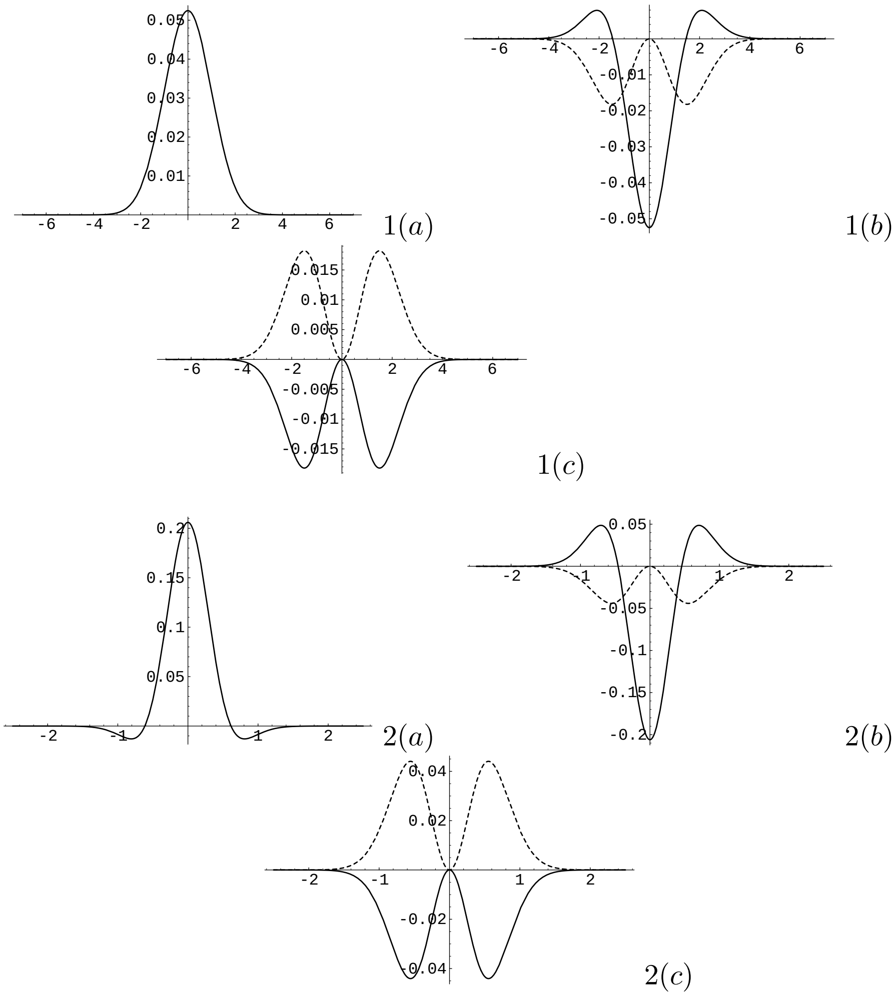

Figure 3: (a) The potential energy E_p; (b) The nonlocal terms E_{nl_1} (firm line) and E_{nl_2} (dashing line); (c) $\mathcal{E}_p$ (dashing line) and $\mathcal{E}_k$ (firm line). 1a,1b and 1c correspond to $k = 0.8$, $\beta = 1/4$, and 2a, 2b and 2c to $k = 0.2$, $\beta = 1/4$

and

$$\mathcal{E}_k = E_{nl_2} \tag{2.23}$$

$$\mathcal{E}_p = E_p + E_{nl_1}\,, \tag{2.24}$$

where E_p and E_{nl_1}, E_{nl_2} are given by (2.15)–(2.17).

On the solution (2.6) we can write explicitly E_p, E_{nl_1} and E_{nl_2} as functions of time. These functions are presented on figure 3 for particular value of parameters $\beta = 1/4$, $k = 0.8$ and $k = 0.2$. Time dependence of $\mathcal{E}_p$ and $\mathcal{E}_k$ is also presented on figure 3

From figure 3c we see that $\mathcal{E}_p \geq 0$ and $\mathcal{E}_k \leq 0$ for $0 \leq t < \infty$. Since the energy is conserved and equal to 0 and the pressure is $2\mathcal{E}_k \leq 0$.

Representing (2.16) and (2.17) as

$$E_{nl_1} = \frac{\beta}{2}\int_0^1 (e^{\beta(1-\frac{\rho}{2})\partial^2}\Phi)(e^{\frac{\beta}{2}\rho\partial^2}\partial^2\Phi)d\rho \tag{2.25}$$

JHEP10(2005)087

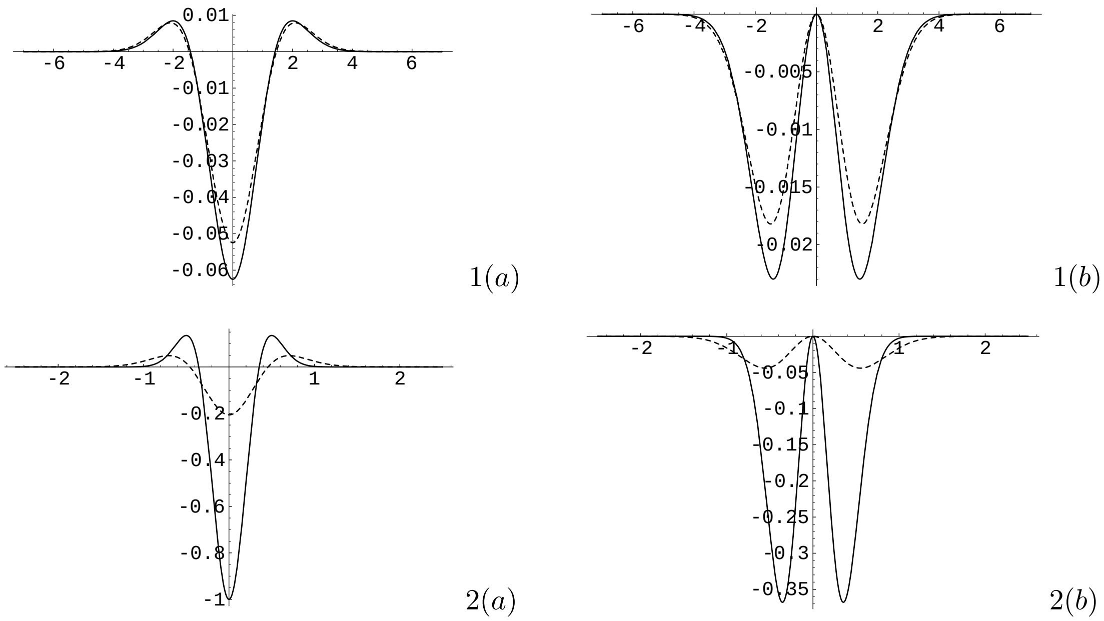

Figure 4: On the left pictures ($1a$ and $2a$) the dashing lines present the exact expressions E_{nl_1} and the firm lines present the approximations to E_{nl_1}. On the right pictures ($1b$ and $2b$) the dashing lines present the exact expressions E_{nl_2} and the firm lines present the approximations to E_{nl_2} . On $1a$ and $1b$ $k = 0.8$, $\beta = 1/4$ and on $2a$ and $2b$ $k = 0.2$, $\beta = 1/4$.

and

$$E_{nl_2} = -\frac{\beta}{2}\int_0^1 ((e^{\beta(1-\frac{\rho}{2})\partial^2}\partial\Phi))(e^{\frac{\beta}{2}\rho\partial^2}\partial\Phi)d\rho. \tag{2.26}$$

we can see that in the approximation neglecting high order derivatives one has

$$E_{nl_2} \sim -\frac{\beta}{2}\dot{\Phi}^2\,, \tag{2.27}$$

$$E_{nl_1} \sim \frac{\beta}{2}\Phi\ddot{\Phi}\,, \tag{2.28}$$

The discrepancy in these approximations are illustrated on the figure 4. We see that the discrepancy becomes smaller when $k \to 1$.

In this approximation

$$\mathcal{E}_k \cong -\frac{\beta}{2}\dot{\Phi}^2 \tag{2.29}$$

$$\mathcal{E}_p \cong -\frac{1}{2}\phi^2 + \frac{\sqrt{k}}{k+1}\Phi^{k+1} + \frac{\beta}{2}\Phi\ddot{\Phi} \tag{2.30}$$

Taking into account that in this approximation

$$-\frac{1}{2}\phi^2 \cong -\frac{1}{2}\Phi^2 - \frac{\beta}{2}\Phi\ddot{\Phi} \tag{2.31}$$

we get

$$\mathcal{E}_p \cong -\frac{1}{2}\Phi^2 + \frac{\sqrt{k}}{k+1}\Phi^{k+1} \equiv V(\Phi)\,. \tag{2.32}$$

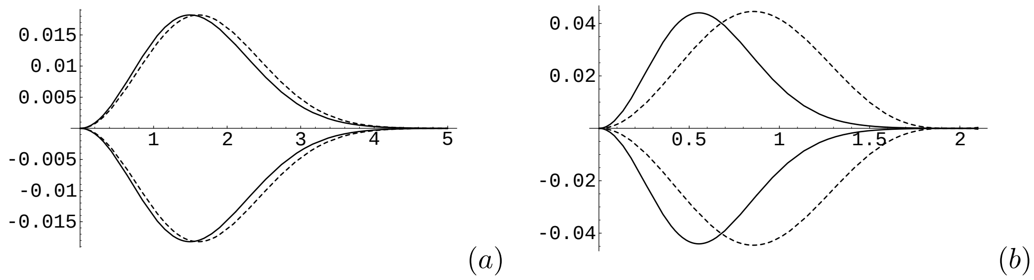

Figure 5: Local kinetic (dashing positive line) and potential (dashing negative line) parts of the energy on zero-energy solutions of eq. (2.11) as functions of time. Nonlocal kinetic (firm negative line) and potential parts (firm positive line) of the energy on the solutions (2.6); the picture for k=0.8 (*a*) and k=0.2 (*b*).

So we see that the approximated kinetic term $\mathcal{E}_k$ (2.29) and potential $\mathcal{E}_p$ (2.32) coincide up to the sign with the kinetic and potential energy for the mechanical problem (2.11).

On figure 5 the kinetic and potential parts of the energy for the local problem (2.11) as functions of time are compared with $\mathcal{E}_k$ and $\mathcal{E}_n$ calculated on the solution (2.6). We see that for $k \to 1$ the kinetic and potential parts for local and nonlocal problems almost coincide for time $0 < t < T_k$.

3. Perturbations of gaussian lump

3.1 Perturbation by the friction

Let us consider the integral equation with the constant friction and time depending coupling constant

$$e^{\beta\partial_t^2+h\partial_t}\Phi_h = \sqrt{k}g(t)\Phi_h^k\,. \tag{3.1}$$

For the case of a special time-depending coupling constant,

$$g(t) = e^{-2h(1-k)t}\,,$$

there is the following lump solution

$$\Phi_h(t) = e^{-\frac{b}{4\beta}t^2+Bt}\,, \qquad B = \frac{h}{2\beta}(-1-\sqrt{1+4\beta b})\,. \tag{3.2}$$

Using the following integral representation

$$e^{\beta\partial_t^2+h\partial_t}\Phi(t) = \frac{1}{\sqrt{4\pi\beta}}\int e^{-\frac{(t-t'+b)^2}{4\beta}}\Phi(t')dt'\,. \tag{3.3}$$

one can check that (3.2) solves (3.1)

Let us consider the mechanical problem with a friction that approximates equation (2.5),

$$\beta\ddot{\varphi}(t) + h\dot{\varphi}(t) + \varphi(t) = g(t)\sqrt{k}\varphi(t)^k\,. \tag{3.4}$$

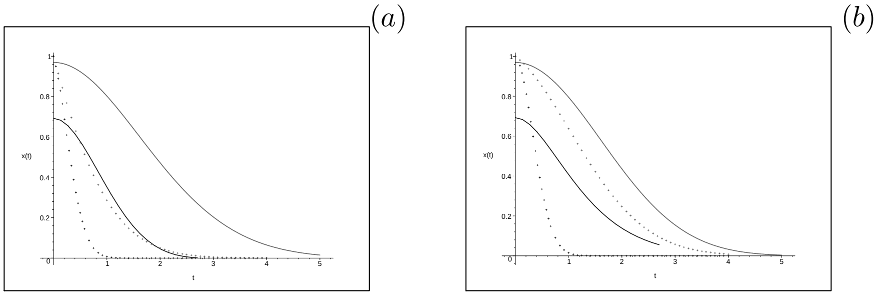

Figure 6: (a) The numerical solution of equation (3.4) for $k = 0.2$ (down solid line) and for $k = 0.8$ (upper solid line) and exact solution to integral equation (2.5) for $\beta = 1/4$ and $k = 0.2$ (down dot line) and $k = 0.8$ (upper dot line), $h = 0.5$; (b) the numerical solution of equation (3.4) for $k = 0.2$ (upper solid line) and for $k = 0.8$ (down solid line) and exact solution to integral equation (2.5) for $\beta = 1/4$ and $k = 0.2$ (down dot line) and $k = 0.8$ (upper dot line), $h = 0.1$.

The particle with the zero energy starts from the point $\varphi_{\max} = (\frac{2\sqrt{k}}{1+k})^{\frac{1}{1-k}}$ and moves to $\varphi_0 = 0$, but do not reach it. The corresponding trajectories are presented in the figure $2b$ for different k and on figure $2c$ are presented the exact lumps (2.6) for different k.

We see that the friction makes behavior of the solutions of the nonlocal equation more closed to that of the corresponding mechanical problem.

3.2 Perturbation by non flat metric

Let us now consider an interaction of the theory (2.1) with the gravity

$$S = \int \sqrt{-g} d^4x \left(\frac{m_p^2}{2} R + \frac{1}{2}\phi^2 - \frac{\sqrt{k}}{k+1}\Phi^{k+1} \right), \tag{3.5}$$

where

$$\Phi = \exp\left(\frac{\beta}{2}\Box_g\right)\phi, \qquad \Box_g = \frac{1}{\sqrt{-g}}\partial_\mu \sqrt{-g} g^{\mu\nu}\partial_\nu . \tag{3.6}$$

On space homogeneous configurations in the Friedmann metric (1.3) the field equation takes the form

$$e^{\beta\mathcal{D}}\Phi(t) = \sqrt{k}\Phi^k(t), \tag{3.7}$$

where $\mathcal{D} = -\partial_t^2 - 3H(t)\partial_t$ and $H(t) = \dot{a}/a$, $\dot{a} = \partial_t a$. The Einstein equations have the form

$$3H^2 = \frac{1}{m_p^2}\rho \tag{3.8}$$

$$H^2 + \frac{2\ddot{a}}{a} = -\frac{1}{m_p^2}p \tag{3.9}$$

with the energy and pressure densities are given by

$$\rho = -\frac{1}{2}(e^{-\frac{\beta}{2}\mathcal{D}})\Phi^2 + \frac{\sqrt{k}}{k+1}\Phi^{k+1} + \mathcal{E}_1 + \mathcal{E}_2 \tag{3.10}$$

$$p = 2\mathcal{E}_2 , \tag{3.11}$$

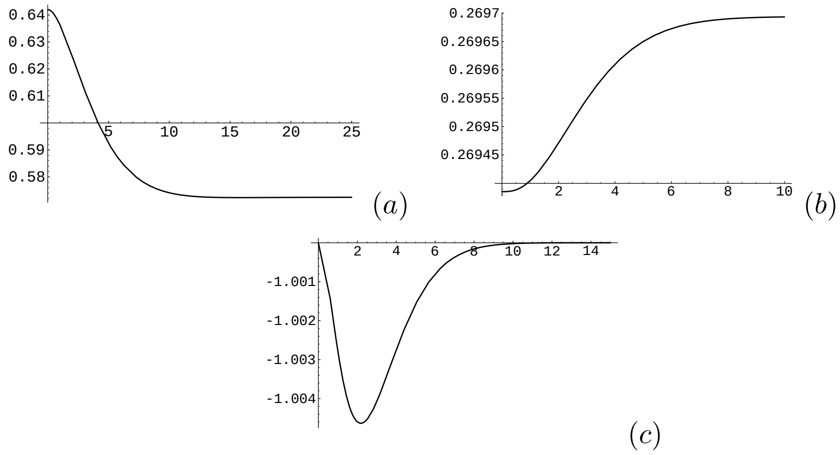

Figure 7: (a) Φ as function on t with the initial condition $\varphi(0) = 0.642$ and $\dot{\varphi}(0) = 0$; (b) function $H = H(t)$ as function on t; (c) $w = w(t)$ as function on t.

where

$$\mathcal{E}_1 = -\frac{\beta}{2}\int_0^1 d\tau (e^{\frac{\beta}{2}\tau\mathcal{D}}\sqrt{k}\Phi^k)\mathcal{D}(e^{-\frac{\beta}{2}\tau\mathcal{D}}\Phi) \tag{3.12}$$

$$\mathcal{E}_2 = -\frac{\beta}{2}\int_0^1 d\tau (e^{\frac{\beta}{2}\tau\mathcal{D}}\partial\sqrt{k}\Phi^k)(e^{-\frac{\beta}{2}\tau\mathcal{D}}\partial\Phi)\,. \tag{3.13}$$

Motivated by the flat case we make the following approximation

$$\exp\left(\partial_t^2 + 3H(t)\partial_t\right)\Phi \approx (\ 1 + \partial_t^2 + 3H(t)\partial_t\ )\ \Phi\,. \tag{3.14}$$

The corresponding Friedmann equations have the form (3.10), (3.11) with

$$\rho = -\frac{1}{2}\dot{\varphi}^2 + V(\varphi)\,, \tag{3.15}$$

$$p = -\frac{1}{2}\dot{\varphi}^2 - V(\varphi) \tag{3.16}$$

and the equation for φ reads

$$\ddot{\varphi} + 3H\dot{\varphi} = V'_{\varphi}\,. \tag{3.17}$$

Here V is given by (2.12)

An numerically solution of the system of equations (3.15) and (3.17) for the potential (2.12) is presented on figure 7.

3.3 Exact gaussian lump solution in Friedman metric

In section 2 we have analyzed the solution for the phantom field with fractional interaction in the Friedman metric. Here we shall construct the potential which leads to exact gaussian lump-type solution (2.6). It is known that if one has an explicit solution for the space-homogeneous scalar field then one can reconstruct the form of potential [34, 23]. To realize this one assumes that the Hubble parameter $H(t)$ has the special form

$$H(t) = W(\phi(t))\,, \tag{3.18}$$

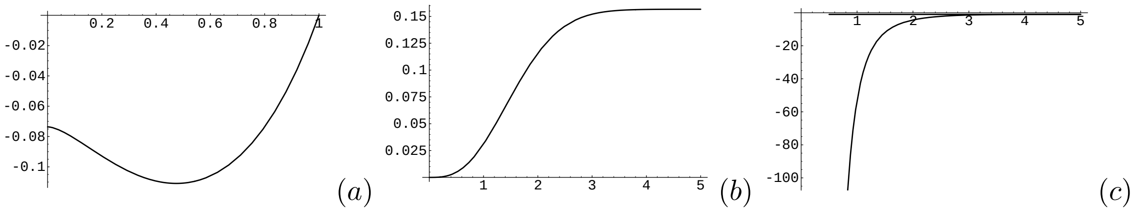

Figure 8: (a) The overturn potential $-V$, (b) $H = H(t)$ as function on t; (c) $w = w(t)$ as function on t and the line $w = -1$

where W is a function called superpotential. Substituting the anzats (3.18) in the Friedmann equation $\dot{H} = \dot{\phi}^2/2m_p^2$ we get

$$2m_p^2 W' = \dot{\phi}\,, \tag{3.19}$$

where prime denotes derivatives in ϕ. For the gaussian lump solutions we have

$$\dot{\phi} = -2\phi\sqrt{-\xi\ \ln\phi}\,, \tag{3.20}$$

that gives the equation

$$2M_p^2 W' = -2\phi\sqrt{-\xi\ \ln\phi}\,, \tag{3.21}$$

from which we reconstruct the superpotential

$$W(\phi) = -\frac{1}{2M_p^2}\phi^2\sqrt{-\xi\log\phi} + \frac{\sqrt{2\pi\xi}}{8m_p^2}\mathrm{erf}(\sqrt{-2\log\phi})\,. \tag{3.22}$$

The potential is obtained from the second Friedmann equation, $V(\phi) = 1/2\dot{\phi}^2 + 3m_p^2W^2$, and

$$V(\phi) = -2\xi\phi^2\,\log\phi + \frac{3\,\xi}{64\,m_p^2}\left(\sqrt{2\,\pi}\,erf(\sqrt{-2\log\phi}) - 4\,\phi^2\,\sqrt{-\log(\phi)}\right)^2 \tag{3.23}$$

The Hubble parameter has the form

$$H(t) = -\frac{1}{8\,m_p^2}\left(4\,t\,\xi e^{-2\xi t^2} - \sqrt{2\,\pi\xi}\,erf(\sqrt{2\xi}\,t)\right). \tag{3.24}$$

The asymptotic behavior of the Hubble parameter and the scale factor are

$$H(t) \sim H_0 = \frac{\sqrt{2\pi\xi}}{8m_p^2}\,, \qquad a(t) \sim e^{H_0 t} \qquad \text{for large } t\,. \tag{3.25}$$

The state parameter has the following explicit form

$$w(t) = -1 - \frac{256\xi t^2 e^{2\xi t^2} m_p^2}{3\left(-4\,t\,\sqrt{\xi} + e^{2\,t^2\,\xi}\,\sqrt{2\,\pi}\,erf(\sqrt{2}\,t\,\sqrt{\xi})\right)^2}\,. \tag{3.26}$$

The shapes of the potential, the Hubble parameter and the state parameter are presented at (figure 8). It is interesting to note that the next to leading term in the asymptotic of (3.26) at large t

$$w(t) \sim -1 - \frac{128\,m_p^2\,t^2\,\xi\,e^{-2\xi t^2}}{3\pi} \tag{3.27}$$

is proportional to m_p^2 meanwhile from the general formula (1.7) one can expect that the deviation from the limiting value -1 could be proportional to $1/m_p^2$. This is caused by a presence of a dependence of m_p^2 in $H_0 \sim 1/m_p^2$ and independence of $\dot{\phi}$ on m_p^2.

4. Hyperbolic Lump

4.1 Numerical construction of the potential

Here we will be interested in the scalar SFT-type nonlocal models described by the following action

$$S = \int d^d x \left[\frac{1}{2}\phi^2 - U(\Phi)\right], \tag{4.1}$$

where U is a polynomial and Φ the smoothed field given by (2.8). Action (4.1) leads to the equation of motion which on the space homogeneous configurations reads

$$e^{\beta\partial_t^2}\Phi = U(\Phi)\,. \tag{4.2}$$

We assume that U has a form

$$U(\Phi) = U_{\vec{\alpha}}(\Phi) \equiv \sum_{n=1}^{N} \frac{\alpha_n}{n+1}\Phi^{n+1}\,, \tag{4.3}$$

We choose a function

$$\Phi_0(t) = \mathrm{sech}^2(t) \tag{4.4}$$

and find the set of coefficients $\{\alpha_n\}$ from a requirement that that a discrepancy

$$\delta_N(\vec{\alpha}) = e^{\beta\partial_t^2}\Phi - U'(\Phi) \tag{4.5}$$

is small in L_2-norm for fixed N, where N is a number of terms in the series (4.3). For numerical calculations we use a representation of the left hand side of (4.2) in term of the integral operator

$$e^{\beta\partial_t^2}\Phi(t) \equiv K[\Phi](t) = \frac{1}{\sqrt{4\pi\beta}}\int\limits_{-\infty}^{\infty} e^{-\frac{(t-\tau)^2}{4\beta}}\,\Phi(\tau)d\tau\,, \tag{4.6}$$

and take $\beta = \frac{1}{4}$. We denote the r.h.s. of (4.2) as a force F

$$F_{\vec{\alpha}}[\Phi] \equiv F_{\alpha_N}[\Phi] = \sum_{n=1}^{N} \alpha_n \Phi^n\,, \tag{4.7}$$

Note that numerical calculations show that we cannot make the discrepancy equal to zero for final N, this illustrate the figure 9a.

Note that already for $N = 5$ the discrepancy is rather small, this illustrate the figure 9b. The coefficients α for different N are presented in the table 2.

It is interesting to note that as follows from the figure 9, there is a tendency of decreasing of the minimum value of the discrepancy when the number of terms in the series (4.3) is increase, moreover the values of the low-order coefficients are stabilized when N is increase.

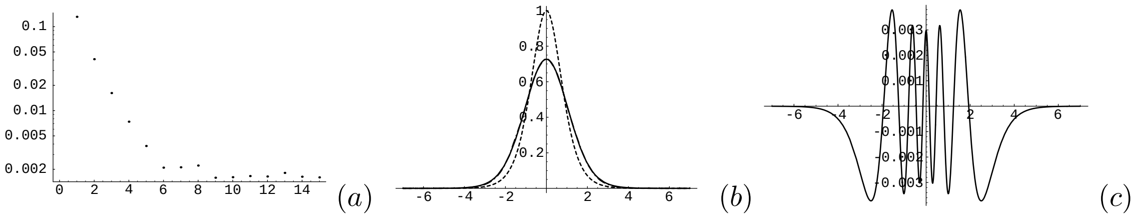

Figure 9: (a) Minimum of the absolute value of the function of discrepancy $\delta_N(\vec{\alpha})$ (4.5) (in *the logarithmic* scale at pintle) depending on number of terms N is presented; $(b)\Phi_0(t) = \mathrm{sech}^2(t)$ is presented by dash line, function $K[\Phi_0](t)$ is presented by the firm line and function $F_{\alpha_5}[\varphi_0]$ is presented by dotdashing line $N = 5$, coefficients α_5 are collected on the table; (c) function $\delta_5(\alpha_5) = K[\varphi_0] - F_{\alpha_5}[\varphi_0]$.

N	α_1	α_2	α_3	α_4	α_5	α_6	α_7
3	1.896	-2.2206	1.0649	-	-	-	-
5	2.319	-5.7831	10.1891	-9.1559	3.1602	-	-
6	2.4309	-7.5998	19.2683	-28.4428	21.4779	-6.4098	-
12	2.4628	-8.2965	23.6528	-38.931	28.6269	0.287057	-6.3996
13	2.4643	-8.3152	23.7106	-38.965	28.5816	0.278636	-6.3756
14	2.4662	-8.3356	23.7655	-38.985	28.5391	0.256198	-6.3702
15	2.4602	-8.2969	23.7264	-39.024	28.5326	0.282346	-6.3252

Table 2: Components of $\vec{\alpha}$ for various N.

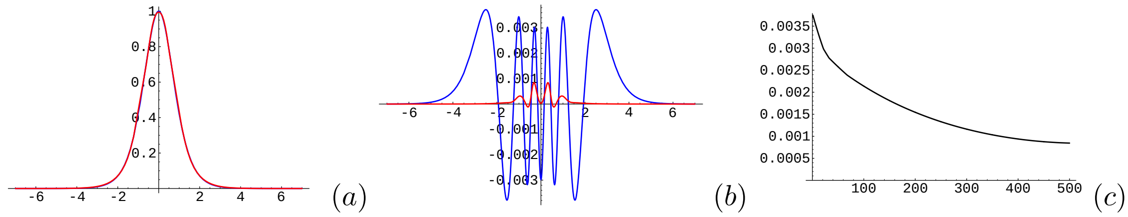

Figure 10: (a) Zero iteration $y_0 = \mathrm{sech}^2(t)$ is depicters by firm line and five hundredth 500 by dashing line($N = 5$); (b)The discrepancy for initial iteration (the line with amplitude 0.003) and for solution $y(t)$ of equation (4.8)(the line with amplitude 0.001); (c)The dependence for descrepansy (4.10) as funcion on number of iteration when the number of terms in the series $N = 5$.

4.2 Numerical solution of the integral equation

We are going to solve the equation

$$K[y](t) = F_{\alpha_N}[y](t)\,, \tag{4.8}$$

where the right hand side is given by F_{α_N}, that minimized the discrepancy for the function (4.4) A solution of this equation we find using the following iteration procedure

$$y_{n+1} = y_n + \lambda(K[y] - F_{\alpha_N}[y])\,, \qquad \lambda = 0.01\,, \tag{4.9}$$

and as the zero approximation we take (4.4), i.e. $y_0 = \mathrm{sech}^2(t)$.

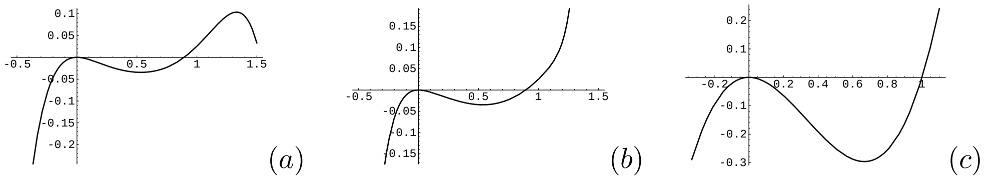

Figure 11: The overturn potential (4.12) when N is equal: (a) $N = 5$ and (b) $N = 14$; (c) the overturn potential $-V_0$.

Numerical calculations show that this iteration procedure converges. A character of a convergent of the iteration procedure is natural to specify by the a maximum of the discrepancy

$$\Delta[y_n] = \max_t |K[y_n](t) - F_{\alpha_N}[y_n](t)| \,. \tag{4.10}$$

As we see that $\Delta[y_n]$ becomes smaller for a large number of iteration n (when the number of terms in the series $N = 5$), however as we can see from figure 10c at $n \sim 500$ $\Delta[y_n]$ goes to a "plateau" and after decreases slowly. The same situation takes place when we consider the case when the number of terms in the series $N = 7, 14, 21, ..etc.$

4.3 Mechanical problem

The mechanical problem that corresponds to (4.8) has the form

$$\beta\ddot{\varphi(t)} = F_\alpha[\varphi] - \varphi \,. \tag{4.11}$$

The potential for this problem is $V_{ot}(\varphi)$

$$V_{ot}(\varphi) = \frac{1}{2}\varphi^2 - U_{\vec{\alpha}}(\varphi) \tag{4.12}$$

$V_{ot}(\varphi)$ is the overturn version of the potential V given by (1.6) with U given by (4.3).

The overturn potentials for N=5 and N=14 are presented on figure 11. It is interesting to note that global forms of corresponding potentials are different for different N see figure 11, but in all considered cases there are local maximum of the potential in the zero field configuration and points of local minimum.

Starting from the zero-energy bounce point, $\varphi(0) = \varphi_0$, where $V(\varphi_0) = 0$, with zero velocity, $\dot{\varphi}(0) = 0$, the particle moves to the local maximum of the potential at the point $\varphi = 0$ during infinite time. For the initial data $\varphi(0) = \varphi_1 < \varphi_0$ and $\dot{\varphi}(0) = 0$ the particle performs a periodic motion. For $\varphi(0) = \varphi_0$ and $\dot{\varphi}(0) \neq 0$ the motion is unbounded.

On figure 11c for a comparison we present the potential $-V_0$. As it is known (see also the subsection 4.5) the lump (4.4) is a zero-energy solution of the mechanical problem with the phantom kinetic term and potential V_0 given by (1.18).

4.4 Energy and pressure

In this subsection similar to the subsection 2.3 we consider the energy and the pressure of the nonlocal problem (4.8) and compare them with energy and pressure of the corresponding mechanical problem (4.11). Equation (4.8) has the conserved energy functional

$$E = E_p + E_{nl_1} + E_{nl_2} \,, \tag{4.13}$$

JHEP10(2005)087

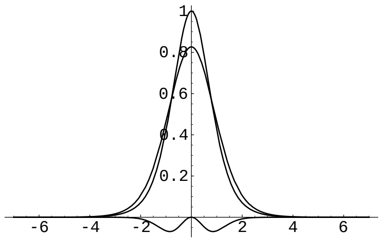

Figure 12: (a) The lump (4.4) and the corresponding smothered function (lowest positive line in the picture) and the pressure (4.18) for $N = 14$ (negative line).

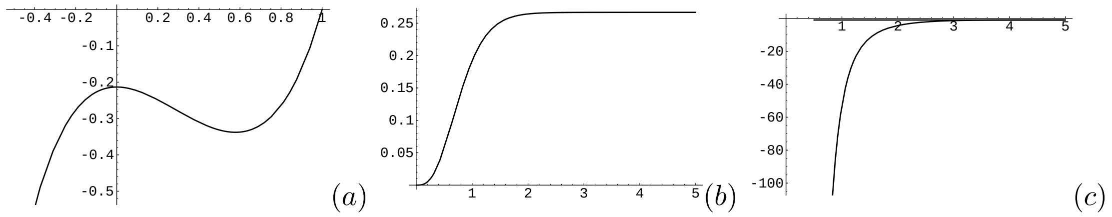

Figure 13: (a)The overturn potential $-V$, (b) $H = H(t)$ as function on t; (c) $w = w(t)$ as function on t.

where

$$E_p = -\frac{1}{2}\phi^2 + U(\Phi), \tag{4.14}$$

$$E_{nl_1} = \frac{\beta}{2}\int_0^1 (e^{-\frac{\beta}{2}\rho\partial^2}U'(\Phi))(e^{\frac{\beta}{2}\rho\partial^2}\partial^2\Phi)d\rho \tag{4.15}$$

and

$$E_{nl_2} = -\frac{a}{2}\int_0^1 ((e^{-\frac{\beta}{2}\rho\partial^2}\partial U'(\Phi)(e^{\frac{\beta}{2}\rho\partial^2}\partial\Phi)d\rho\,. \tag{4.16}$$

The pressure

$$P = E_{nl_2} - E_p - E_{nl_1} \tag{4.17}$$

has the representation (4.17) and

$$P = -a\int_0^1 (e^{(2-\rho)\frac{\beta}{2}\partial^2}\partial\Phi)(e^{\frac{\beta}{2}\rho\partial^2}\partial\Phi)d\rho\,. \tag{4.18}$$

4.5 Exact lump solution in Friedmann metric

In the full analogy with what has been done in section 3.3 we can easily find a potential for which the function (4.4) is a solution to the Friedmann equations. It has the form

$$V(\phi) = 2\,(1-\phi)\,\phi^2 - \frac{4\,(-1+\phi)^3\,(2+3\,\phi)^2}{75\,{m_p}^2}\,. \tag{4.19}$$

The shape of the potential is presented at figure 13a.

The Hubble parameter has the form

$$H(t) = \frac{2\,(4+\cosh(2\,t))\,\operatorname{sech}(t)^2\tanh(t)^3}{15\,{m_p}^2} \tag{4.20}$$

and its shape is presented on (figure 13b. $H(t)$ and the scale factor $a(t)$ have the following asymptotic behavior at large t

$$H(t) \sim \frac{2}{15 m_p^2}\,, \qquad a(t) \sim e^{\frac{4}{15 m_p^2} t} \qquad \text{for t} \quad \to \infty. \tag{4.21}$$

The state parameter is given by the following explicit formula

$$w(t) = -1 - \frac{75\, m_p^2 \coth(t)^4}{(4 + \cosh(2\,t))^2} \tag{4.22}$$

and we see that for large times $w(t)$ goes to -1.

Acknowledgments

We would like to thank Ya. Volovich for help with numerical calculations. This work is supported in part by RFBR grant 05-01-00578 and INTAS grant 03-51-6346. I.A. is also supported by the grant for scientific schools. L.J. is also financially supported by the fellowship of the "Dynasty" Foundation and International Center for Fundamental Physics in Moscow, by the grant of the "Russian Science Support Foundation", and by the personal grant from Swedish Institute.

References

[1] A. Sen, *Rolling tachyon*, *JHEP* **04** (2002) 048 [hep-th/0203211]; *Tachyon matter*, *JHEP* **07** (2002) 065 [hep-th/0203265]; *Tachyon dynamics in open string theory*, hep-th/0410103.

[2] G.W. Gibbons, *Thoughts on tachyon cosmology*, *Class. and Quant. Grav.* **20** (2003) S321 [hep-th/0301117].

[3] A.V. Frolov, L. Kofman and A.A. Starobinsky, *Prospects and problems of tachyon matter cosmology*, *Phys. Lett.* **B 545** (2002) 8 [hep-th/0204187];
G.N. Felder, L. Kofman and A. Starobinsky, *Caustics in tachyon matter and other Born-Infeld scalars*, *JHEP* **09** (2002) 026 [hep-th/0208019].

[4] V. Sahni and Y. Shtanov, *Braneworld models of dark energy*, *JCAP* **11** (2003) 014 [astro-ph/0202346];
P. Brax, C. van de Bruck and A.C. Davis, *Brane world cosmology*, *Rept. Prog. Phys.* **67** (2004) 2183–2232 [hep-th/0404011];
B. McInnes, *The phantom divide in string gas cosmology*, *Nucl. Phys.* **B 718** (2005) 55 [hep-th/0502209].

[5] I.Y. Aref'eva, *Nonlocal string tachyon as a model for cosmological dark energy*, astro-ph/0410443.

[6] Supernova Cosmology Project collaboration, S. Perlmutter et al., *Measurements of omega and lambda from 42 high-redshift supernovae*, *Astrophys. J.* **517** (1999) 565 [astro-ph/9812133].

JHEP10(2005)087

[7] Supernova Search Team collaboration, A.G. Riess et al., *Observational evidence from supernovae for an accelerating universe and a cosmological constant*, *Astron. J.* **116** (1998) 1009–1038 [astro-ph/9805201];
Supernova Search Team collaboration, A.G. Riess et al., *Type ia supernova discoveries at z¿1 from the hubble space telescope: evidence for past deceleration and constraints on dark energy evolution*, *Astrophys. J.* **607** (2004) 665 [astro-ph/0402512].

[8] The Supernova Cosmology Project collaboration, R.A. Knop et al., *New constraints on ω_m, ω_λ and w from an independent set of eleven high-redshift supernovae observed with HST*, *Astrophys. J.* **598** (2003) 102 [astro-ph/0309368].

[9] SDSS collaboration, M. Tegmark et al., *Cosmological parameters from SDSS and WMAP*, *Phys. Rev.* **D 69** (2004) 103501 [astro-ph/0310723].

[10] WMAP collaboration, D.N. Spergel et al., *First year wilkinson microwave anisotropy probe (wmap) observations: determination of cosmological parameters*, *Astrophys. J. Suppl.* **148** (2003) 175 [astro-ph/0302209].

[11] V. Sahni, *Dark matter and dark energy*, *Lect. Notes Phys.* **653** (2004) 141–180 [astro-ph/0403324].

[12] P. Frampton, *Dark energy - a pedagogic review*, astro-ph/0409166.

[13] R.R. Caldwell, *A phantom menace?*, *Phys. Lett.* **B 545** (2002) 23 [astro-ph/9908168].

[14] B. McInnes, *The dS/CFT correspondence and the big smash*, *JHEP* **08** (2002) 029 [hep-th/0112066].

[15] R.R. Caldwell, M. Kamionkowski and N.N. Weinberg, *Phantom energy and cosmic doomsday*, *Phys. Rev. Lett.* **91** (2003) 071301 [astro-ph/0302506].

[16] V.K. Onemli and R.P. Woodard, *Super-acceleration from massless, minimally coupled ϕ^4*, *Class. and Quant. Grav.* **19** (2002) 4607 [gr-qc/0204065];
V.K. Onemli and R.P. Woodard, *Quantum effects can render $w < -1$ on cosmological scales*, *Phys. Rev.* **D 70** (2004) 107301 [gr-qc/0406098].

[17] S.M. Carroll, M. Hoffman and M. Trodden, *Can the dark energy equation-of-state parameter w be less than -1?*, *Phys. Rev.* **D 68** (2003) 023509 [astro-ph/0301273].

[18] A. Melchiorri, L. Mersini-Houghton, C.J. Odman and M. Trodden, *The state of the dark energy equation of state*, *Phys. Rev.* **D 68** (2003) 043509 [astro-ph/0211522].

[19] T. Padmanabhan, *Cosmological constant: the weight of the vacuum*, *Phys. Rept.* **380** (2003) 235 [hep-th/0212290].

[20] B. Feng, X.L. Wang and X.M. Zhang, *Dark energy constraints from the cosmic age and supernova*, *Phys. Lett.* **B 607** (2005) 35 [astro-ph/0404224];
B. Feng, M. Li, Y.S. Piao and X. Zhang, *Oscillating quintom and the recurrent universe*, astro-ph/0407432.

[21] S. Nojiri, S.D. Odintsov and S. Tsujikawa, *Properties of singularities in (phantom) dark energy universe*, *Phys. Rev.* **D 71** (2005) 063004 [hep-th/0501025].

[22] W. Fang, H.Q. Lu, Z.G. Huang and K.F. Zhang, *Phantom cosmology with the Born-Infeld type scalar field*, hep-th/0409080.

[23] I.Y. Aref'eva, A.S. Koshelev and S.Y. Vernov, *Exactly solvable SFT inspired phantom model*, astro-ph/0412619.

[24] S.M. Carroll, V. Duvvuri, M. Trodden and M.S. Turner, *Is cosmic speed-up due to new gravitational physics?*, *Phys. Rev.* **D 70** (2004) 043528 [astro-ph/0306438];
A.D. Dolgov and M. Kawasaki, *Can modified gravity explain accelerated cosmic expansion?*, *Phys. Lett.* **B 573** (2003) 1 [astro-ph/0307285];
M.E. Soussa, R.P. Woodard, *The force of gravity from a lagrangian containing inverse powers of the Ricci scalar*, *Gen. Rel. Grav.* **36** (2004) 855;
G. Allemandi, A. Borowiec and M. Francaviglia, *Accelerated cosmological models in first-order non-linear gravity*, *Phys. Rev.* **D 70** (2004) 043524 [hep-th/0403264]; *Accelerated cosmological models in Ricci squared gravity*, *Phys. Rev.* **D 70** (2004) 103503 [hep-th/0407090];
J.W. Moffat, *Modified gravitational theory as an alternative to dark energy and dark matter*, astro-ph/0403266;
J.D. Barrow, *Sudden future singularities*, *Class. and Quant. Grav.* **21** (2004) L79 [gr-qc/0403084];
M.C.B. Abdalla, S. Nojiri and S.D. Odintsov, *Consistent modified gravity: dark energy, acceleration and the absence of cosmic doomsday*, *Class. and Quant. Grav.* **22** (2005) L35 [hep-th/0409177].

[25] E. Witten, *Noncommutative geometry and string field theory*, *Nucl. Phys.* **B 268** (1986) 253; *Interacting field theory of open superstrings*, *Nucl. Phys.* **B 276** (1986) 291.

[26] V.A. Kostelecky and S. Samuel, *Spontaneous breaking of Lorentz symmetry in string theory*, *Phys. Rev.* **D 39** (1989) 683.

[27] P. West, *The spontaneous compactification of the closed bosonic string*, *Phys. Lett.* **B 548** (2002) 92 [hep-th/0208214].

[28] I.Y. Arefeva, P.B. Medvedev and A.P. Zubarev, *Background formalism for superstring field theory*, *Phys. Lett.* **B 240** (1990) 356;
C.R. Preitschopf, C.B. Thorn and S.A. Yost, *Superstring field theory*, *Nucl. Phys.* **B 337** (1990) 363;
I.Y. Arefeva, P.B. Medvedev and A.P. Zubarev, *New representation for string field solves the consistence problem for open superstring field*, *Nucl. Phys.* **B 341** (1990) 464.

[29] N. Berkovits, A. Sen and B. Zwiebach, *Tachyon condensation in superstring field theory*, *Nucl. Phys.* **B 587** (2000) 147 [hep-th/0002211].

[30] I.Y. Aref'eva, A.S. Koshelev, D.M. Belov and P.B. Medvedev, *Tachyon condensation in cubic superstring field theory*, *Nucl. Phys.* **B 638** (2002) 3 [hep-th/0011117]; *Gauge invariance and tachyon condensation in cubic superstring field theory*, *Nucl. Phys.* **B 638** (2002) 21 [hep-th/0107197].

[31] K. Ohmori, *A review on tachyon condensation in open string field theories*, hep-th/0102085.

[32] I.Y. Arefeva, D.M. Belov, A.A. Giryavets, A.S. Koshelev and P.B. Medvedev, *Noncommutative field theories and (super)string field theories*, hep-th/0111208.

[33] W. Taylor, *Lectures on D-branes, tachyon condensation and string field theory*, hep-th/0301094.

[34] O. DeWolfe, D.Z. Freedman, S.S. Gubser and A. Karch, *Modeling the fifth dimension with scalars and gravity*, *Phys. Rev.* **D 62** (2000) 046008 [hep-th/9909134].

[35] I.Y. Aref'eva, L.V. Joukovskaya and A.S. Koshelev, *Time evolution in superstring field theory on non-BPS brane, I. Rolling tachyon and energy-momentum conservation*, *JHEP* **09** (2003) 012 [hep-th/0301137];
I.Ya. Aref'eva, *Rolling tachyon in NS string field theory*, *Fortschr. Phys.* **51** (2003) 652;
I.Ya. Aref'eva and L.V. Joukovskaya, *Rolling Tachyon on non-BPS brane*, Lectures given at the II Summer School in Modern Mathematical Physics, Kopaonik, Serbia, 1–12 Sept. 2002.

[36] N. Moeller and B. Zwiebach, *Dynamics with infinitely many time derivatives and rolling tachyons*, *JHEP* **10** (2002) 034 [hep-th/0207107].

[37] L. Brekke, P.G.O. Freund, M. Olson and E. Witten, *Nonarchimedean string dynamics*, *Nucl. Phys.* **B 302** (1988) 365.

[38] Y. Volovich, *Numerical study of nonlinear equations with infinite number of derivatives*, *J. Phys.* **A 36** (2003) 8685 [math-ph/0301028].

[39] V.S. Vladimirov and Y.I. Volovich, *On the nonlinear dynamical equation in the p-adic string theory*, *Theor. Math. Phys.* **138** (2004) 297 [math-ph/0306018].

[40] K. Ohmori, *Toward open-closed string theoretical description of rolling tachyon*, *Phys. Rev.* **D 69** (2004) 026008 [hep-th/0306096].

[41] L. Joukovskaya and Y. Volovich, *Energy flow from open to closed strings in a toy model of rolling tachyon*, math-ph/0308034.

[42] V. Forini, G. Grignani and G. Nardelli, *A new rolling tachyon solution of cubic string field theory*, hep-th/0502151.

[43] L. Bonora, C. Maccaferri, R.J. Scherer Santos and D.D. Tolla, *Exact time-localized solutions in vacuum string field theory*, *Nucl. Phys.* **B 715** (2005) 413 [hep-th/0409063].

[44] H. Hata and S. Moriyama, *Boundary and midpoint behaviors of lump solutions in vacuum string field theory*, *Phys. Rev.* **D 72** (2005) 046004 [hep-th/0504184].

JHEP10(2005)087